FORMULATION, CHARACTERIZATION, AND TYROSINASE INHIBITORY ASSAYS OF NIACINAMIDE-LOADED NANOPARTICLE GEL AS A SKIN WHITENING AGENT

RISA AHDYANI[1]*, NOR LATIFAH[1], HAYATUS SA'ADAH[1], ERLINA FATMASARI[1], IRFAN ZAMZANI[1]

Faculty of Pharmacy, University of Muhammadiyah Banjarmasin, South Borneo, Indonesia
*Corresponding author: Risa Ahdyani; *Email: risaahdyani@umbjm.ac.id

ABSTRACT

Objective: This research aims to formulate a nanoparticle gel of Niacinamide (N) using Chitosan (C) and Sodium Alginate (SA) and determine its tyrosinase inhibitory activity as a skin whitening.

Methods: N nanoparticle was carried out using C (0.01%), SA (0.1%), and Calcium Chloride (CC 0.25 %). N was incorporated into the nanoparticle system by different concentrations in each Formula (F): F1(2.5 %), F2 (5%), F3 (7.5%), and F4 (10%). Each formula was characterized for particle size, Polydispersity Index (PI), and Zeta potential by Zetasizer, entrapment efficiency using Spectrophotometer Uv-Vis, and molecular structure using Fourrier Transform Infrared (FTIR). Then, Hydroxy Propyl Methyl Cellulose (HPMC) was incorporated to form a nanoparticle gel of N. N-loaded nanoparticle gel was determined tyrosinase inhibitory using L-tyrosine to obtain Inhibitory Concentration of 50 (IC_{50}) value. Furthermore, data was analyzed using one-way ANOVA (p-value<0.05).

Results: The particle size, PI, Zeta potential, and entrapment efficiency obtained for all formulations were found to be F1 (217±7.21 nm, 0.49±0.0521,+8.24±1.75 mV, and 61.22±2.88 %); F2 (225±11.37 nm, 0.51±0.0246,+9.12± 1.97 mV, and 64.01±4.12%); F3 (289±15.26 nm, 0.26±0.0152,+10.55± 1.56 mV, and 68.71±3.86 %); F4 (428±9.44 nm, 0.38±0.0347, 12.33±1.80 mV, and 72.59±3.01%) respectively. The result of FTIR spectra indicated N-loaded in the nanoparticles system. Tyrosinase inhibitory activity of N-loaded gel nanoparticles obtained IC_{50} 99.9775, 73.5605, 52.7187, and 42.3145 µg/ml, respectively.

Conclusion: N-loaded nanoparticle gel was successfully prepared and could be a promising candidate for skin whitening agent.

Keywords: Niacinamide, Gel, Nanoparticle, Tyrosinase, Whitening skin

INTRODUCTION

Beauty standards are ideal characteristics specifically of a woman's beauty that a socially constructed normative standards. Some examples of beauty standards are body shape, skin tone, height, facial features, hairstyles, clothing styles, and body weight. These are subjects to change over time which is dependent on time or era. Each era has different preferences for women's physical attractiveness that constructed certain beauty standards. Different countries and societies also have completely different perceptions of women's physical attractiveness that are anchored in society and ideologies. Skin tone is one of the beauty standards for women's physical attractiveness. White skin has become the heart of Asian beauty standards influenced by various cultures and arts in many Asian countries such as China, Korea, Japan, and India. Asian women are obsessed with skin whitening products to whiten their skin tone. Skin tone can make a clear line between rich and poor. White colour skin means living a comfortable life away from the scorching sun during hard work. This assumption corresponds to the physical aspect of Asians where the first signs of aging on Asian skin are pigments such as freckles, not wrinkles like Westerners. Therefore, white skin colour is not only for beautifying but also becomes the value to keep skin looking younger [1].

The standard of beauty set by society often puts pressure on women themselves. Moreover, this led to many women seeming eager so hard to fulfill the existing beauty standard in their society. Some women willingly perform changes to their facial features and bodies to fulfill their desire to be beautiful, indeed according to their ideals. Over the years, the consumption of cosmetic products has been increasing rapidly due to the increase in awareness of beauty and aesthetics among consumers around the world, especially female consumers. As a result, the woman started investing more in their appearance and look. The U. S. Food and Drug Administration (FDA), which regulates cosmetics in the United States defines cosmetics as products "intended to be applied to the human body for cleansing, beautifying, promoting attractiveness, or altering the appearance

without affecting the body's structure or functions." Woman have been using cosmetics at different periods in their lives during childhood or adolescence which play a greater role in enhancing their beauty and self-confidence. Nowadays, the awareness of using cosmetics is increasing due to high exposure to social media which impacts consumer buying behavior. Many studies were conducted to find out that the most influencing factor in to use of cosmetics was skin concerns [2, 3].

There are many cosmetic products on the market to beautify the appearance, including products with claims to whiten the skin or are called skin whitening [4]. Skin whitening is influenced by several factors, one of which is melanin synthesis which can cause dark skin colour if it is produced excessively. Tyrosinase expression plays a role in melanin synthesis and determines human skin colour. Thus, tyrosinase inhibition becomes a mechanism for skin whitening. Among the whitening cosmetic products circulating in Indonesia contain Niacinamide (N). N can reduce melanogenesis in the skin by inhibiting tyrosinase. Based on previous clinical testing, 5% of N can inhibit melanosomes by 35-68%, which is characterized by a significant reduction in skin hyperpigmentation and an increase in skin brightness after 4 w of use [5].

N is chemically known as pyridine-3-carboxamide which can be delivered to specific areas of the skin as a percutaneous administration route. However, there is a major challenge represented by the stratum corneum as a skin barrier that can prevent several molecules from penetrating into the skin. It is also highly dependent on active pharmaceutical ingredients' physicochemical properties. N is a small molecule with a molecular weight of 122.1 Da, extremely water soluble, and has a log p value of-0.37. Thus, those properties are not ideal characteristics for delivering substance as percutaneous delivery [6]. The nanotechnology delivery system is a novel approach to improve percutaneous delivery of N, in which biopolymer nanoparticles are explored in this study. The biopolymer is a polymer molecule that has been used extensively as biomaterials in nanoparticle delivery

systems. It has a lot of advantages due to its properties, such as being biocompatible, non-toxic, non-irritant, and forming a network of particle matrices. The preparation of the biopolymer system uses double polymer which has opposite charges to form a matrix for entrapping drug molecules. Biopolymeric nanoparticles are biodegradable nanoparticles that are mostly used and made of natural polymer-like polysaccharides, such as Chitosan (C) and Sodium Alginate (SA) [7]. C and SA are great combinations of biopolymers that can be used in nanotechnology delivery systems through controlled drug release profiles [8]. It can be prepared by ionic gelation methods through an interaction mechanism based on the negative charge of the uronic acid carboxylic groups of SA with the positive surface charge of the protonated amino groups of C. The formation of C-SA nanoparticles by the ionic gelation method produces a pre-gel that consists of very small aggregates of gel particles, which are then followed by the addition of a polycationic solution to form the polyelectrolyte complex [9]. The C-SA nanoparticles can protect drug encapsulation from enzymatic degradation, deliver the drug to target organs, prolong the contact time of active ingredients with target epithelial cells, and control drug release [10, 11]. Biopolymeric nanoparticle attempts to improve the permeation of drug molecules into the skin. It is also useful for cosmeceutical formulation due to sustained release properties that facilitate prolonged dermal therapy [12]. It is well established that cosmeceutical products formulated with small particle sizes are trending among consumers, as the nanoparticle system supports a better permeation of bioactive ingredients through stratum corneum [13]. Nanoparticle gel is a promising

strategy for maximizing the transportation of pharmacological components to the stratum corneum as a skin barrier [14]. Therefore, nanoparticle gel of C-SA loaded N has many advantages in the drug delivery system through the skin and it is expected to be a promising product as a skin whitening agent.

MATERIALS AND METHODS

Materials

N was purchased from Merck (Germany), C low molecular weight (50 kDa to 190 kDa) was purchased from Sigma Aldrich (Germany), SA was purchased from Sigma Aldrich (Darmstadt, Germany), CC was purchased from Merck (Germany), glacial acetic acid, hydrochloric acid, and sodium hydroxide were purchased from Merck (New Jersey, USA). HPMC was purchased (Germany) and deionized water was purchased from Brataco, kojic acid powder, L-tyrosine substrate, and potassium dihydrogen phosphate.

Methods

Preparation of N-loaded nanoparticle gel

The nanoparticle of N was prepared based on ionic gelation researched by Nurkhasanah et 2015. The amount of N, C, SA, and CC were weighted and dissolved into each medium to form an aqueous phase in a ratio of 1:1:1:1. N was mixed into SA and homogenized using vortex for 30 seconds and then added CC. C was also mixed into that mixture and homogenized for 30 seconds to form N nanoparticles [15].
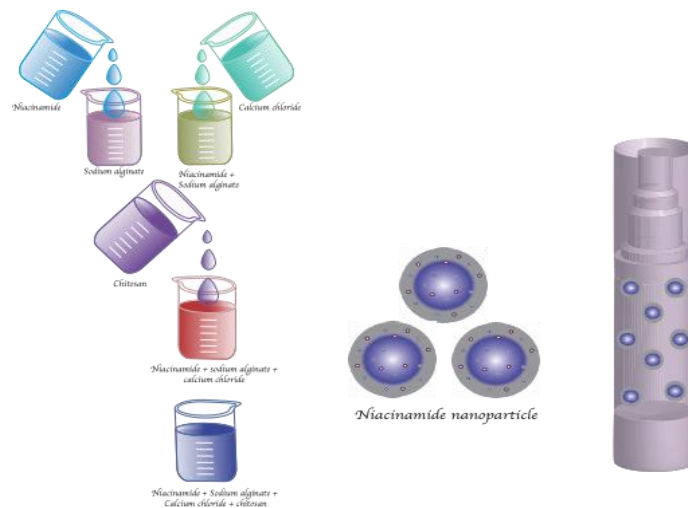

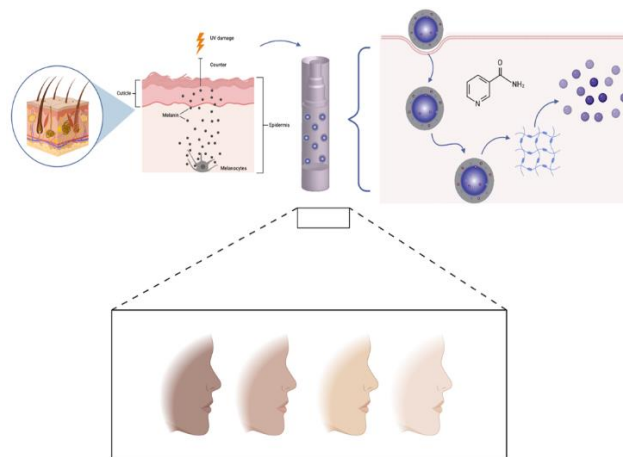**Fig. 1: Illustration of formulation for N-loaded nanoparticle gel**

Fig. 2: Illustration of mechanism for N-loaded nanoparticle gel as a skin whitening agent

Characterization of NC nanoparticles

Measurement of particle size, polydispersity index, and zeta potential

The particle size, polydispersity index, and Zeta potential of N nanoparticles were analyzed by the method of dynamic light scattering (DLS). The N nanoparticles were examined using Zetasizer Nano ZS (Malvern, UK). A certain amount of sample was dispersed in 5 ml of aquadest and then placed in the disposable cuvette. Replications were done for each measurement of the same samples for 3 times. This instrument was controlled with Malvern software [16].

Structure characterization

Structure characterization of N nanoparticles was analyzed using a Fourrier Transform Infra-Red (FTIR) spectrophotometer (Thermo Scientific Nicolet iS10, Madison, WI). This instrument was controlled with Omnic software. The measurements were done in the middle infrared region of 4000-650 cm-1. Replications were done for 3 times.

Measurement of entrapment efficiency

N nanoparticles were measured indirectly. The sample was ultra-centrifuged (Velocity 18R) at 15000 rpm for 30 min at 4 °C to separate unloaded N nanoparticles. The amount of unloaded N nanoparticles was analyzed using using UV-Vis spectrophotometer [17, 18] (Thermo Scientific Genesys 10S UV) at 265 nm [19]. The following equation was used to calculate entrapment efficiency.

$$\% \text{ Entrapment efficiency} = \frac{\text{Total amount of N} - \text{unload nanoparticle of N}}{\text{Total amount of N}} \times 100$$

Formulation of N-loaded nanoparticles gel

An amount of 1.5 g HPMC was incorporated into N nanoparticles and then stirred to form a homogenous gel of N-loaded nanoparticles. Then, the physicochemical properties of the nanoparticle gel of N were characterized. N was incorporated into the nanoparticle system in different concentrations (F1= 2.5 %, F2 = 5%, F3= 7.5%, and F4 =10% respectively).

Preparation of phosphate buffer (0.05 M, pH 6.5)

An amount of 3.402 g of KH_2PO_4 (MW= 136.09 g/mol) was weighed and then dissolved into 450 ml of CO_2-free distilled water. The pH value was adjusted to 6.5 by adding 1 M NaOH solution approximately 25 ml. Then added CO_2 free distilled water up to 500 ml [18].

Preparation of tyrosinase enzyme solution 333 Units/ml

The concentration of tyrosinase solution used in the activity inhibition test Tyrosinase was 333 Units/ml [20]. An amount of 5 mg (5771 Units/mg) of tyrosinase was weighed, then put into a 5.0 volumetric flask ml, dissolved with 50 mmol phosphate buffer pH 6.5. Soluble tyrosinase has an activity of 5771 Units/ml and it was used as a stock solution. The stock solution was pipetted as much as 577 μl, then put into a 10.0 ml volumetric flask, so that it was obtained tyrosinase with activity of 333 Units/ml. Tyrosinase solution (333 Units/ml) and solution Tyrosinase stock (5771 Units/ml) were stored at-20 °C [21].

Preparation of kojic acid solution

An amount of 5 mg of kojic acid powder was weighed, put into a 10.0 measuring flask ml, dissolved in 50 mmol phosphate buffer solution pH 6.5, to obtain a solution of kojic acid with a concentration of 500 μg/ml. Then, 5.0 ml of kojic acid solution 500 μg/ml was pipetted then put into a 10.0 ml volumetric flask, obtaining a concentration of 250 μg/ml. Next, dilution was carried out until kojic acid solution of 125; 62.5; 31.25; 15.625; and 7.8125 μg/ml as a concentration variation to obtain the IC_{50} value [21].

Inhibitory tyrosinase assays

Tyrosinase inhibition assays were performed with L-tyrosine as substrate. The reaction mixture (1000 μl) contained 685 μl of phosphate buffer (0.05 M, pH 6.5), 15 μl of mushroom tyrosinase (2500 U ml−1), 200 μl of NC gel nanoparticles, and 100 μl of 5 mmolL-tyrosine. After the addition of L-L-tyrosine reaction was immediately monitored at 492 nm for dopachrome formation in the reaction mixture using a microplate reader. Kojic acid was used as a positive control. The concentrations of NC gel nanoparticles used for the mushroom tyrosinase inhibition assay were 20, 40, 60, 80, and 100 mg/ml. Each measurement was made in triplicate [21].

Statistical analysis

The percentage of inhibition was calculated by the equation:

$$\% \text{ Inhibition} = \frac{A-B}{A} \times 100\% \text{ .... (1)}$$

A = Absorbance of blank

B = Absorbance of sample

The IC50 value, a concentration giving 50 % inhibition of tyrosinase activity determined by interpolation of concentration (ln)-response curves and substituted y value to 50. One-way ANOVA was used to analyze the tyrosinase inhibitory activity of at a 95% confidence level [21].

Table 1: The result of particle diameter (nm), PI, Zeta potential (mV), and entrapment efficiency (%)

Formula	Particle diameter (nm)	PI	Zeta potential (mV)	Entrapment efficiency (%)
F1	217±7.21	0.49±0.0521	+8.24±1.75	61.22±2.88
F2	225±11.37	0.51±0.0246	+9.12±1.56	64.01±4.12
F3	289±15.26	0.26±0.0152	+10.55±1.97	68.71±3.86
F4	428±9.44	0.38±0.0347	+12.33±1.80	72.59±3.01

F1: Formulation 1 (NC = 2.5 %), F2: Formulation 2 (NC = 5 %), F3: Formulation 3 (NC = 7.5 %), F4: Formulation 4 (NC = 10 %). Data is expressed as a mean±SD (n=3) and significantly different (P<0.05) using one-way ANOVA.

RESULTS AND DISCUSSION

Measurement of particle size, PI, Zeta potential, and entrapment efficiency

The particle size is a critical factor in the preparation of nanoparticles. N was incorporated into the nanoparticle system in different concentrations (2.5 %, 5%, 7.5%, and 10%, respectively). All formulas showed results of particle size in nanometres within the range of 200-430 nm. This result is similar to a previous study by [6] that formulated nano gel-loaded N using carrageenan and polyvinylpyrrolidone polymers combined with jojoba oils as permeation enhancers and obtained particle sizes ranging from 133 and 320 nm. Hyun and coworkers also reported that hybrid C and N-coupled ZnO nanoparticle has particle sizes ranging from 90-100 nm [22]. The result was analyzed using one-way ANOVA and showed significant differences (P<0.05) for particle size of N-loaded gel Nanoparticle with different concentrations (F1 = 2.5%; F2= 5%; F3=7.5%; and F4= 10%).

Based on the result, there was also a noticeable rise in particle size as the N concentration increased. The previous study reported that increasing concentration from active ingredient caused increasing in particle size [17]. Notably, the particle size was found to increase as long with increasing of N due to the increase in the viscosity of the organic phase. Then, it renders solvent diffusion more difficult and results in larger nanoparticle size [23]. Sahudin *et al.*, 2022 reported also the particle sizes of β-arbutin C nanoparticles (0.1–0.6%)

increase as the concentration of β-arbutin increases. Particle size in nanometres could penetrate into the skin deeply and remain within the stratum corneum for up to 10 days. Furthermore, small diameter particles penetrated better into human skin which is evaluated using biopsies and analyzed the histological sections of the skin. It is also suitable for drug percutaneous delivery. Hence, the small particle produces good stability due to the effect of Brownian motion being dominant over gravitational force [24].

The Zeta potential is one of the important evaluations used to determine the stability of colloidal dispersion systems [25]. It describes the electrokinetic potential of particles within nanoparticles as the potential difference between shear location due to the tightly bound surface layer and bulk solution [26]. It indicates also the stability of nanoparticles due to aggregation probability based on the Derjaguin, Landau, Verwey, dan Overbeek (DLVO) theory. The Van der Waals attraction and the electrostatic repulsion force are two forces that contribute to the stability of the nanosystem. The stability of nanoparticles will exist due to great particle charge that prevents aggregation based on electrostatic repulsion forces. Therefore, strong electrostatic repulsion forces among particles can prevent aggregation and improve nanoparticle stability [27, 28]. When it approaches 0 mV, the repulsion of interparticulate is reduced and colloidal dispersion becomes less stable due to particles that can approach one another to interact and form aggregates. It becomes a sign of lower colloidal dispersion stability [29, 30]. A high value of Zeta potential indicates a high repulsion force among particles due to electrostatic force, which is related proportionally to the Zeta potential of particles obtained. Thus, a high value of zeta potential can lead to a more stable nanoparticle [31].

The Zeta potential values obtained for all formulas were found to be+8.24±1.75,+9.12±1.56,+10.55±1.97, and+12.33±1.80 mV respectively, and positively charged (table 1). The result was analyzed using one-way ANOVA and showed significantly different (P<0.05) for Zeta potential values of NC-loaded gel nanoparticles with different concentrations (F1 = 2.5%; F2= 5%; F3=7.5%; and F4= 10%). The positive charge on the surface of the particle is related to the formation of nanoparticles through the ionic gelation mechanism. It is influenced by the composition of the formula and dispersion medium [32]. The protonated amino groups (NH₃+) of C and amide groups of N are neutralized by the negative charge of polymeric SA. All formulas showed positive Zeta potential, which indicated that positively charged particles of carboxylic groups of SA were sufficiently neutralized by the protonated amino groups (NH₃+) of C and amide groups of N. This result was following the previous study reported that the Zeta potential value is strongly influenced by the availability of protonated amino groups (NH₃+) originating C that was neutralized by carboxylic groups of SA [33].

The polydispersity index (PI) or heterogeneity index is a parameter to describe the non-uniformity of particle size distribution obtained. It is a number calculated from two parameters that fit the correlation data and are dimensionless. The PI value is smaller than 0.5 and has uniformity of particle size distribution or is called monodisperse which is not easier to settle and form aggregation [25]. Particle size distribution is uniform as the smaller PI is produced. Meanwhile, the PI value is greater than 0.7 and has a broad particle size distribution [24]. Several studies also report that a PI value is more than 0.5 indicates a broad particle size distribution that impacts the properties of particles. Therefore, the increasing PI value could impact the forming aggregate and lead to instability of the nanoparticle system [31]. Basto *et al.* 2021 studied nano gel-loaded N that exhibited a fairly narrow size distribution and monodisperse with a PI value ≤ 0.3 [6].

All formulas showed entrapment efficiency values ranging from 61.22 % to 72.59 % as observed in table 1. A maximum entrapment efficiency of 72.59 % was attained at an N concentration of 10%. This result showed higher entrapment efficiency than a previous study reported by Basto *et al.*, 2021 that formulated hybrid nanogel of N using carrageenan and polyvinylpyrrolidone polymers combined with jojoba oils as permeation enhancers obtained loading capacity ranging from 5.3-7.6 % [6]. Based on table 1, it was observed that the entrapment efficiency increased significantly upon increasing the concentration of N. Increasing of N concentration in the formula increased the availability of the binding site in the system. This result was in agreement with Kalam *et al.*, 2016 reported that the availability of the binding sites for the crosslinker increased, hence higher entrapment efficiency percentage [34]. This result was in accordance with a study reported by Salatin *et al.* 2021 that encapsulation efficiency was enhanced as the number of bioactive ingredients increased [23]. It was also reported by Khan *et al.* 2022 that increasing the amount of drug resulted increasing in entrapment efficiency [8]. Furthermore, Aboosabaa *et al.* 2021 also reported that higher entrapment efficiency was confirmed by the increase in particle size; contrarily decreasing entrapment efficiency resulted in a significant reduction of particle size [35]. The result was analyzed using one-way ANOVA and showed significantly different (P<0.05) for entrapment efficiency values of N Loaded Gel Nanoparticle with different concentrations (F1 = 2.5%; F2= 5%; F3=7.5%; and F4= 10%).

FTIR analysis

The FTIR spectra could be used to get information about molecular structure from the vibration of functional groups at a certain wavenumber [13]. The FTIR spectra of N nanoparticles are shown in fig. 3.
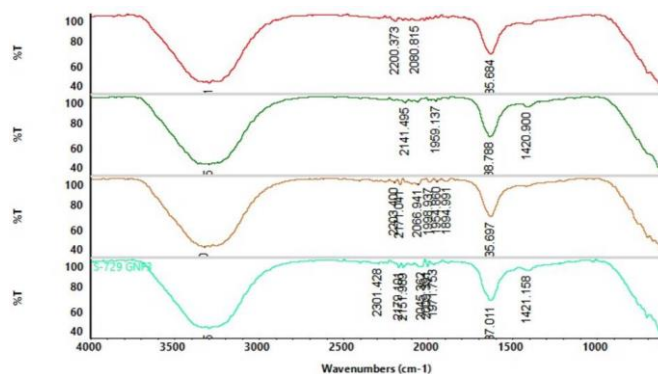

Fig. 3: The spectra of NC-loaded gel nanoparticle

The FTIR spectra of N nanoparticles in fig. 3 indicate the interaction among nanoparticle components. C indicates broadband appearing at 3354 cm-1 due to the stretching vibrations of O-H/N-H. The peak at 2873 cm-1 is due C-H stretching vibrations. The band for C≡C stretching vibrations appears at 2113.39 cm-1. The weak peak at 1645 cm-1 is due to C=N stretching vibrations. The peak at 1419.57

cm-1 is due to O-H bending vibrations. The C-O stretching vibrations appear at wavenumber 1149.91 cm-1, 1061.63 cm-1, and 1025.46 cm-1, respectively. The peak at 894.14 cm-1 is due to C-H bending vibrations. Meanwhile, SA indicates a broadband appearing at 3357 cm-1 due to O-H stretching vibrations. The band for C≡C stretching vibrations appears at 2099.39 cm-1. The peak at 1597.67 cm-1 is

due to C=C stretching vibrations. The peak at 1409.45 cm-1 appears due to O-H bending vibrations. The C-O stretching vibrations appear at wavenumber 1295.48 cm-1 and 1086.80 cm-1, respectively. The peak at 882.52 cm-1 is due to C-H bending vibrations. The C-H stretching vibrations appear at wavenumber 3039.76 cm-1, 2964.64 cm-1, 2890.35 cm-1, and 2852.60 cm-1, respectively. Meanwhile, the C-H bending vibrations appear at wavenumber 1980.62 cm-1. The peaks at wavenumber 1702.20 cm-1is due to C=O stretching vibrations. The C=N stretching vibrations appear at wavenumber 1618.42 cm-1. There are peaks at 1489.02 and 1448.64 cm-1 due to the N-H bending and O-H bending vibrations. The peak at wavenumber 1380.43 cm-1 is due to S-N vibrations. Peaks indicate the C-O stretching vibrations at wavenumber 1292.88 cm-1, 1262.02 cm-1, 1227.27 cm-1, 1197.37 cm-1, 1054.22 cm-1, respectively. The C=C bending vibrations appears at wavenumber 988.17 cm-1, 954.49 cm-1, 890.02 cm-1, 861.08 cm-1, and 806.50 cm-1, respectively. After loading niacinamide in the nanoparticles, there is broadband at wavenumber 3354.92 cm-1 due to O-H stretching vibrations. The band for C≡C stretching vibrations appears at wavenumber 2106.60 cm-1. Both of these peaks are similar to the peak of chitosan and sodium alginate. There is a sharp peak at wavenumber 1603.44 cm-1 due to C=N stretching vibrations. The peaks at 1416.91 cm-1 are due to O-H bending vibrations. The peaks indicate the C-O stretching vibrations at wavenumber 1076.31 cm-1 and 1026.10 cm-1, respectively. These peaks are also similar to the peaks of C and SA. There are peaks at wavenumber 888.67 cm-1 and 817.51 cm-1 due to C=C bending vibrations. These peaks are similar to the peak of niacinamide. These results confirmed the characterization of the nanoparticle component, which indicated N loaded in the nanoparticle system.

Inhibitory tyrosinase assays

Inhibitory tyrosinase assays is a test based on inhibition of dopachrome product formation that results from the reaction of the L-tyrosine enzyme. Inhibition of dopachrome product formation is characterized by a decrease in colour intensity as measured by using a microplate reader at a maximum wavelength of 492 nm. Microplate reader is a spectrophotometry method that passes light at certain wavelengths crossing the plate containing the sample and then measures the transmission of light intensity to obtain an absorbance of the sample. The absorbance is used for calculating the magnitude of inhibiting L-tyrosine reaction [21]. This assay was carried out using kojic acid as a positive control to compare the IC_{50} value obtained and the IC_{50} value of the standard. It is also a compound that is widely used of whitening products in the market. Furthermore, it has good stability in cosmetic products. Based on the table 6, it was obtained IC_{50} value for F1=99.9775; F2=73.5605; F3= 52.7187; and F4= 42.3145 µg/ml, respectively. Then, it was analyzed using one-way ANOVA and showed significantly different (P<0.05) for IC_{50} value of NC-loaded gel nanoparticles with different concentrations (F1 = 2.5%; F2= 5%; F3=7.5%; and F4= 10%). Inhibitory tyrosinase assays of N 10% loaded gel nanoparticles showed the lowest IC_{50} value approaching positive control of kojic acid as 19.3869 µg/ml. Therefore, NC-loaded nanoparticle gel was successfully prepared and could be a promising candidate for skin whitening agents. According to the result of a study by Lin *et al.* 2012 that measured the inhibitory activity of tyrosinase of N used L-tyrosine as a substrate and obtained an IC_{50} value of 151.3 mmol [36]. Li *et al.* 2022 reported that the evaluated anti-melanogenic effect of nicotinamide-stabilized nanocrystal obtained tyrosinase activity and melanin content decreased to 62.97%±0.52% and 36.57%±0.44%, respectively [37]. This result was accordance in study by Hakozaki *et al.* 2002 that reported the mechanism of N as skin whitening through reduced melanosome transfer from melanocytes to surrounding keratinocytes in a coculture system [5]. Wohlrab and Kreft 2014 also reported N works as skin whitening by blocking the reversible transfer of melanosomes from melanocytes into keratinocytes through inhibition of keratinocyte factor [38].
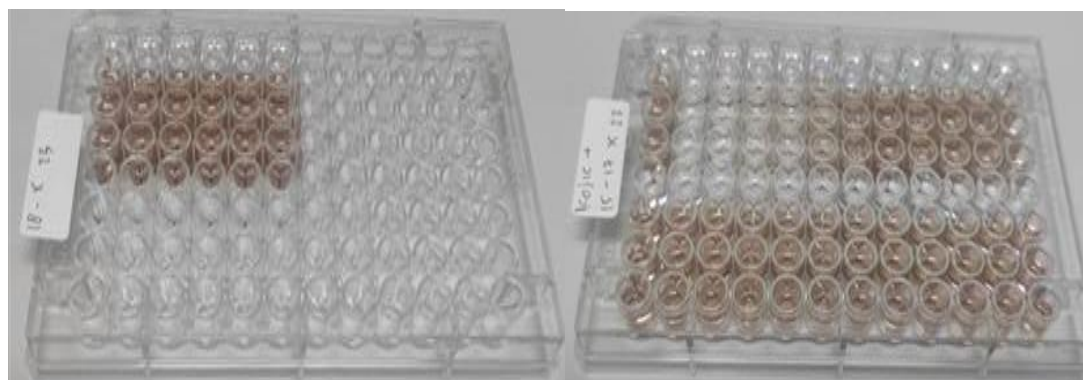

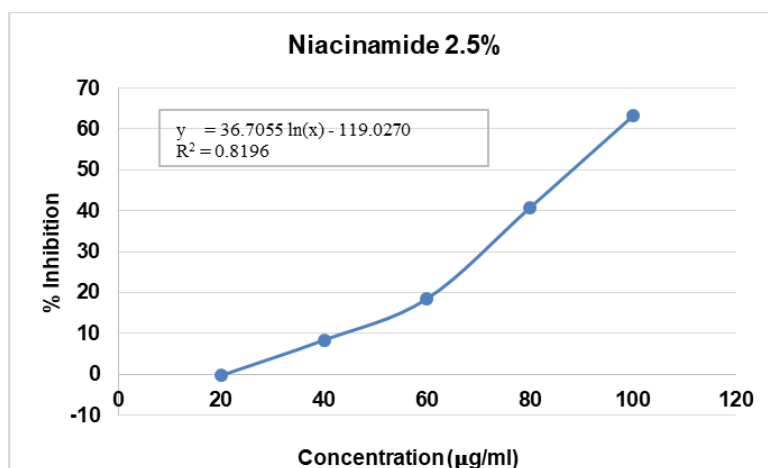**Fig. 4: Inhibitory tyrosinase assays using microplate reader**

Fig. 5: Graphic of inhibitory tyrosinase of N 2.5% loaded gel nanoparticles

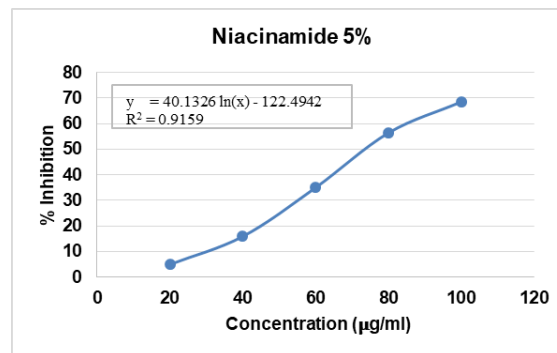**Table 2: Inhibitory tyrosinase assays of N 2.5% loaded gel nanoparticles**

Replication	Concentration (µg/ml)				
	100	**80**	**60**	**40**	**20**
R1	0.216	0.343	0.475	0.526	0.574
R2	0.212	0.339	0.472	0.528	0.582
R3	0.211	0.346	0.467	0.535	0.583
% Inhibition					
R1	62.6298	40.6574	17.8201	8.9965	0.6920
R2	63.3218	41.3495	18.3391	8.6505	-0.6920
R3	63.4948	40.1384	19.2042	7.4394	-0.8651
x̄±SD	63.1488	40.7151	18.4544	8.3622	-0.2884

Information: R1: Replication 1, R2: Replication 2, R3: Replication 3, x̄: mean, SD: Standard deviation, (n=3)

Table 3: Inhibitory tyrosinase assays of N 5% loaded gel nanoparticles

Replication	Concentration (µg/ml)				
	100	**80**	**60**	**40**	**20**
R1	0.184	0.246	0.377	0.488	0.551
R2	0.179	0.252	0.371	0.483	0.549
R3	0.183	0.258	0.379	0.487	0.548
% Inhibition					
R1	68.1661	57.4394	34.7751	15.5709	4.6713
R2	69.0311	56.4014	35.8131	16.4360	5.0173
R3	68.3391	55.3633	34.4291	15.7439	5.1903
x̄± SD	68.5121	56.4014	35.0058	15.9170	4.9596

Information: R1: Replication 1, R2: Replication 2, R3: Replication 3, x̄: mean, SD: Standard deviation, (n=3)

Fig. 6: Graphic of inhibitory tyrosinase of N 5% loaded gel nanoparticles

Table 4: Inhibitory tyrosinase assays of N 7.5% loaded gel nanoparticles

Replication	Concentration (µg/ml)				
	100	**80**	**60**	**40**	**20**
R1	0.124	0.196	0.307	0.375	0.462
R2	0.121	0.182	0.311	0.373	0.456
R3	0.123	0.198	0.312	0.38	0.451
% Inhibition					
R1	78.5467	66.0900	46.8858	35.1211	20.0692
R2	79.0657	68.5121	46.1938	35.4671	21.1073
R3	78.7197	65.7439	46.0208	34.2561	21.9723
x̄± SD	78.7774	66.7820	46.3668	34.9481	21.0496

Information: R1: Replication 1, R2: Replication 2, R3: Replication 3, x̄: mean, SD: Standard deviation, (n=3)

Table 5: Inhibitory tyrosinase assays of N 10% loaded gel nanoparticles

Replication	Concentration (µg/ml)				
	100	**80**	**60**	**40**	**20**
R1	0.091	0.152	0.277	0.314	0.402
R2	0.099	0.15	0.271	0.317	0.411
R3	0.095	0.159	0.274	0.316	0.412
% Inhibition					
R1	84.2561	73.7024	52.0761	45.6747	30.4498
R2	82.8720	74.0484	53.1142	45.1557	28.8927
R3	83.5640	72.4913	52.5952	45.3287	28.7197
x̄± SD	83.5640	73.4141	52.5952	45.3864	29.3541

Information: R1: Replication 1, R2: Replication 2, R3: Replication 3, x̄: mean, SD: Standard deviation, (n=3)
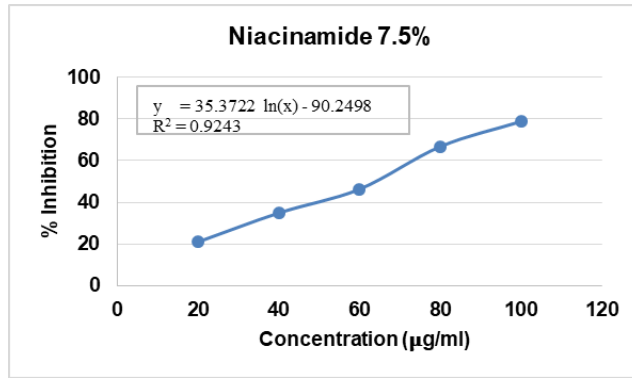
Fig. 7: Graphic of inhibitory tyrosinase of N 7.5% loaded gel nanoparticles
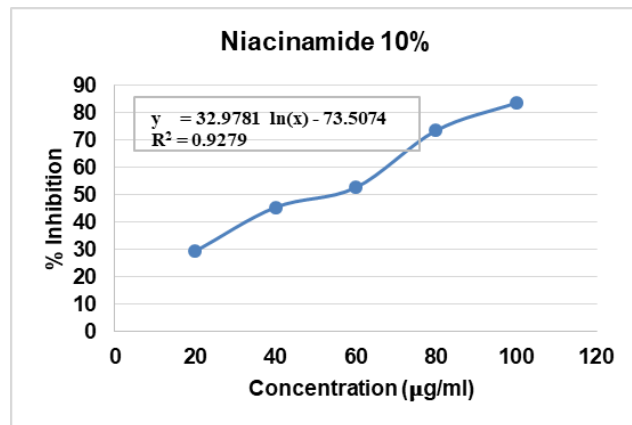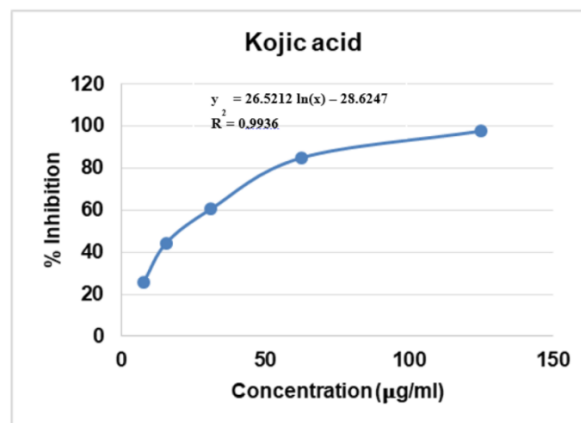

Fig. 8: Graphic of inhibitory tyrosinase of N 10% loaded gel nanoparticles

Table 6: Inhibitory tyrosinase assays of kojic acid

Replication	Concentration (µg/ml)				
	7.8125	15.625	31.25	62.5	125
R1	0.45	0.359	0.266	0.138	0.065
R2	0.457	0.351	0.271	0.144	0.075
R3	0.459	0.358	0.27	0.136	0.076
% Inhibition					
R1	26.866	43.843	61.194	85.075	98.881
R2	25.560	45.336	60.261	83.955	97.015
R3	25.187	44.030	60.448	85.448	96.828
x̄± SD	25.871	44.403	60.634	84.826	97.575

Information: R1: Replication 1, R2: Replication 2, R3: Replication 3, x̄: mean, SD: Standard deviation, (n=3)

Fig. 9: Graphic of inhibitory tyrosinase of kojic acid

Table 10: IC$_{50}$ value of N-loaded gel nanoparticle

Sample	IC$_{50}$ (µg/ml)
NC 2.5%	99.9775
NC 5%	73.5605
NC 7.5%	52.7187
NC 10%	42.3145
Kojic acid	19.3869

Information: One-way Anova test (Normal Data) and Kruskal Wallis Test (abnormal data) were carried out to see any differences or changes of tyrosinase inhibitory activity of NC-loaded gel nanoparticle

CONCLUSION

We have prepared successfully N-loaded nanoparticle gel by ionic gelation using a double biopolymer of C and SA, and CC as a stabilizer. N was incorporated into the nanoparticle system in different concentrations F1 (2.5 %), F2 (5%), F3 (7.5%), and F4 (10%), respectively. The particle size, PI, Zeta potential, and entrapment efficiency obtained for all formulations were found to be F1 (217±7.21 nm, 0.49±0.0521,+8.24±1.75 mV, and 61.22±2.88 %); F2 (225±11.37 nm, 0.51±0.0246,+9.12± 1.97 mV, and 64.01±4.12%); F3 (289±15.26 nm, 0.26±0.0152,+10.55± 1.56 mV, and 68.71±3.86 %); F4 (428±9.44 nm, 0.38±0.0347, 12.33±1.80 mV, and 72.59±3.01%) respectively. The result of FTIR spectra indicated N-loaded in the nanoparticles system. Tyrosinase inhibitory activity of N-loaded gel nanoparticles obtained IC$_{50}$ 99.9775, 73.5605, 52.7187, and 42.3145 µg/ml, respectively. Finally, we concluded that N-loaded nanoparticle gel was successfully prepared and could be a promising candidate for skin whitening agents.

ACKNOWLEDGMENT

AUTHORS CONTRIBUTIONS

RA designed research, analyzed data, and did critical thinking on the manuscript. NL, HS, EF, and IZ compiled data and prepared a manuscript.

CONFLICT OF INTERESTS

The author declares there is no conflict of interest

REFERENCES

1. Chuklin P, NA Ranong S, Juntaramontee K, Charoenrat C, Prohmvitak S. Perception on Asian beauty standard: a global perspective. ASEAN International Sandbox Conferences; 2023. http://aseansandbox.org.
2. Lakshmi VV, Radhika V, Munje G. Purchase pattern of skin care products among women. Biological Forum an International Journal. 2022;15(1):356-66.
3. Mahalakshmi K, Geetha B, Prasad S. Consumers buying behavior towards cosmetics among women with reference to Coimbatore City. J Manag Entrep. 2024;17(2 (XVI)):35-43.
4. Soyata A, Chaerunnisa AY. Whitening agent: mekanisme, sumber dari alam dan teknologi formulasinya. Majalah Farmasetika. 2021;6(2):169-86. doi: 10.24198/mfarmasetika.v6i2.28139.
5. Hakozaki T, Minwalla L, Zhuang J, Chhoa M, Matsubara A, Miyamoto K. The effect of niacinamide on reducing cutaneous pigmentation and suppression of melanosome transfer. Br J Dermatol. 2002;147(1):20-31. doi: 10.1046/j.1365-2133.2002.04834.x, PMID 12100180.
6. Basto R, Andrade R, Nunes C, Lima SA, Reis S. Delivery of niacinamide to skin using hybrid nanogels enhances photoprotection effect. Pharmaceutics Topical; 2021. doi: 10.3390/pharmaceutics, PMID 34834883.
7. Gharat S, Ghadge A, Phalak SD, Bodke V, Gavand A, Ganvir D. A review on template synthesis of nanoparticle. Int J Pharm Pharm Sci. 2024;16(5):22-9. doi: 10.22159/ijpps.2024v16i5.50661.
8. Khan S, Dubey N, Khare B, Jain H, Jain PK. Preparation and characterization of alginate chitosan crosslinked nanoparticles bearing drug for the effective management of ulcerative colitis. Int J Curr Pharm Sci. 2022;14(5):48-61. doi: 10.22159/ijcpr.2022v14i5.2040.
9. Azevedo MA, Bourbon AI, Vicente AA, Cerqueira MA. Alginate/chitosan nanoparticles for encapsulation and controlled release of vitamin B2. Int J Biol Macromol. 2014;71:141-6. doi: 10.1016/j.ijbiomac.2014.05.036, PMID 24863916.
10. Nalini T, Basha SK, Mohamed Sadiq AM, Kumari VS, Kaviyarasu K. Development and characterization of alginate/chitosan nanoparticulate system for hydrophobic drug encapsulation. J Drug Deliv Sci Technol. 2019;52:65-72. doi: 10.1016/j.jddst.2019.04.002.
11. Emami J, Boushehri MS, Varshosaz J. Preparation, characterization and optimization of glipizide controlled release nanoparticles. Res Pharm Sci. 2014;9(5):301-14. PMID 25657802.
12. El-Feky GS, El-Banna ST, El-Bahy GS, Abdelrazek EM, Kamal M. Alginate coated chitosan nanogel for the controlled topical delivery of silver sulfadiazine. Carbohydr Polym. 2017;177:194-202. doi: 10.1016/j.carbpol.2017.08.104, PMID 28962758.
13. Gupta V, Mohapatra S, Mishra H, Farooq U, Kumar K, Ansari MJ. Nanotechnology in cosmetics and cosmeceuticals-a review of latest advancements. Gels. 2022;8(3):1-31. doi: 10.3390/gels8030173, PMID 35323286.
14. Karanam M, Gottemukkula L. A review of nanogels as novel drug delivery systems. Asian J Pharm Clin Res. 2023;16(4):10-7. doi: 10.22159/ajpcr.2023.v16i4.46790.
15. Yuwono T, Nurani LH, Rizki MI, Kraisintu DK. The development of chitosan nanoparticles from *Hibiscus sabdariffa l* calyx extract from Indonesia and Thailand. Nurkhasanah Int J Pharm Sci Res. 2015;6(5):1855-61. doi: 10.13040/IJPSR.0975-8232.6(5).1855-61.
16. Xie X, Tao Q, Zou Y, Zhang F, Guo M, Wang Y. PLGA nanoparticles improve the oral bioavailability of curcumin in rats: characterizations and mechanisms. J Agric Food Chem. 2011;59(17):9280-9. doi: 10.1021/jf202135j, PMID 21797282.
17. Gautham U, Patil A, Hemanth G. Formulation and evaluation of nanoparticle drug delivery system for treatment of hypertension. Int J App Pharm. 2023;15(6):90-7. doi: 10.22159/ijap.2023v15i6.48971.
18. Jyothi D, Priya S, James JP. Development and optimization of polymeric nanoparticles of glycyrrhizin: physicochemical characterization and antioxidant activity. Int J App Pharm. 2024;16(1):166-71. doi: 10.22159/ijap.2024v16i1.49164.
19. Altunay N. Optimization of ultrasound-assisted dispersive liquid–liquid microextraction of niacinamide in pharmaceutical and cosmetic samples using experimental design. Microchem J. 2021;170. doi: 10.1016/j.microc.2021.106659.
20. Batubara I, Darusman LK, Mitsunaga T, Rahminiwat M, Djauhari E. Potency of Indonesian medicinal plants as tyrosinase inhibitor and antioxidant agent. J of Biological Sciences. 2010;10(2):138-44. doi: 10.3923/jbs.2010.138.144.
21. Sagala Z, Ripaldo F. Inhibitory of tyrosinase enzym activity assay and antioxidant activity assay of Harendong (*Melastoma malabathricum* L.) ethanol extract *in vitro*. Indonesia Natural Research Pharmaceutical Journal. 2020;5(1). doi: 10.52447/inspj.v5i1.1800.
22. Jo HJ, Joo SM, Kim JY, Yu KH, Kim SW. Development of a hybrid chitosan and niacinamide-coupled ZnO nanoparticle composite

for sun protection application. Nanomater. 2019;2019:1-9. doi: 10.1155/2019/5957606.

23. Salatin S, Barar J, Barzegar Jalali MB, Adibkia K, Kiafar F, Jelvehgari M. An alternative approach for improved entrapment efficiency of hydrophilic drug substance in PLGA nanoparticles by interfacial polymer deposition following solvent displacement. Jundishapur J Nat Pharm Prod. 2018;13(4):e12873. doi: 10.5812/JJNPP.12873.

24. Sahudin S, Sahrum Ayumi N, Kaharudin N. Enhancement of skin permeation and penetration of β-arbutin fabricated in chitosan nanoparticles as the delivery system. Cosmetics. 2022;9(6). doi: 10.3390/cosmetics9060114.

25. Raditya I, Effiniora A, Mahdi J. Preparasi nanogel verapamil hidroklorida menggunakan metode gelasi ionik antara kitosan-natrium tripolifosfat sebagai sediaan antihipertesi. J Farmasi Indones. 2013;6:201-10.

26. Liu BR, Chan MH, Chen HH, Lo SY, Huang YW, Lee HJ. Chapter 3 Mandraccia L, Slavin G. editors. Effects of surface charge and particle size of cell-penetrating peptide/nanoparticle complexes on cellular internalization in cell membrane. New York: Nova Science Publishers; 2013.

27. Danaei M, Dehghankhold M, Ataei S, Hasanzadeh Davarani F, Javanmard R, Dokhani A. Impact of particle size and polydispersity index on the clinical applications of lipidic nanocarrier systems. Pharmaceutics. 2018;10(2). doi: 10.3390/pharmaceutics10020057, PMID 29783687.

28. Honary S, Zahir F. Effect of zeta potential on the properties of nano-drug delivery systems-a review (Part 1). Trop J Pharm Res. 2013;13(2):255. doi: 10.4314/tjpr.v12i2.19.

29. Benamer Oudih S, Tahtat D, Nacer Khodja A, Mahlous M, Hammache Y, Guittoum AE. Chitosan nanoparticles with controlled size and zeta potential. Polym Eng Sci. 2023;63(3):1011-21. doi: 10.1002/pen.26261.

30. Antoniou J, Liu F, Majeed H, Qi J, Yokoyama W, Zhong F. Physicochemical and morphological properties of size controlled chitosan tripolyphosphate nanoparticles. Colloids and Surfaces A: Physicochemical and Engineering Aspects. 2015;465:137-46. doi: 10.1016/j.colsurfa.2014.10.040.

31. Pham DT, Saelim N, Tiyaboonchai W. Design of experiments model for the optimization of silk fibroin-based nanoparticles. Int J App Pharm. 2018;10(5):195-201, doi: 10.22159/ijap.2018v10i5.28139.

32. Sumathi R, Tamizharasi S, Sivakumar T. Formulation and evaluation of polymeric nanosuspension of naringenin. Int J App Pharm. 2017;9(6):10-5. doi: 10.22159/ijap.2017v9i6.21674.

33. Morsi N, Ghorab D, Refai H, Teba H. Preparation and evaluation of alginate/chitosan nanodispersions for ocular delivery. Int J Pharm Pharm Sci. 2015;7:234-40.

34. Abul Kalam MA, Khan AA, Khan S, Almalik A, Alshamsan A. Optimizing indomethacin-loaded chitosan nanoparticle size, encapsulation, and release using Box–Behnken experimental design. Int J Biol Macromol. 2016;87:329-40. doi: 10.1016/j.ijbiomac.2016.02.033, PMID 26893052.

35. Abosabaa SA, ElMeshad AN, Arafa MG. Chitosan nanocarrier entrapping hydrophilic drugs as advanced polymeric system for dual pharmaceutical and cosmeceutical application: a comprehensive analysis using box-behnken design. Polymers. 2021;13(5):1-16. doi: 10.3390/polym13050677, PMID 33668161.

36. Lin YS, Chen SH, Huang WJ, Chen CH, Chien MY, Lin SY. Effects of nicotinic acid derivatives on tyrosinase inhibitory and antioxidant activities. Food Chem. 2012;132(4):2074-80. doi: 10.1016/j.foodchem.2011.12.052.

37. Li Y, Xiang H, Xue X, Chen Y, He Z, Yu Z. Dual antimelanogenic effect of nicotinamide-stabilized phloretin nanocrystals in larval zebrafish. Pharmaceutics. 2022;14(9):1-14. doi: 10.3390/pharmaceutics14091825, PMID 36145574.

38. Wohlrab J, Kreft D. Niacinamide-mechanisms of action and its topical use in dermatology. Skin Pharmacol Physiol. 2014;27(6):311-5. doi: 10.1159/000359974, PMID 24993939.